Weather-Forecast-Linked Energy Management for PV-Assisted Mobile Base Stations in the Philippines

1st Junliang XIAO
Dept. of X-tech development
NTT DOCOMO, INC.
Tokyo, Japan
junliang.xiao.tb@nttdocomo.com

2nd Masaki NAKAMURA
Dept. of X-tech development
NTT DOCOMO, INC.
Tokyo, Japan
nakamura.masaki.ua@nttdocomo.com

***Abstract*—This paper presents a field demonstration of weather-forecast-linked energy management for a photovoltaic (PV)-assisted mobile base station in the Philippines. The method uses next-day weather forecasts to prepare lithium-ion battery (LiB) charging headroom before high PV generation is expected, enabling the site to absorb surplus solar energy while retaining battery functionality for base-station operation. The demonstration system consisted of a 7.38 kW PV array, a 6 kW PV converter, a 3840 Ah LiB bank, a rectifier with 52.5 V output voltage and 44 A output current, an energy-management server, and an approximately 2.31 kW telecom load. One-minute field logs from a 26-day demonstration period were evaluated. The operational PV self-sufficiency index was estimated at 38.11% under a no-LiB counterfactual and 61.18% with LiB-enabled surplus capture. The LiB captured 332.60 kWh of surplus PV energy. To validate the predictive control basis, forecast-derived surplus opportunities were compared with hourly measured surplus occurrence. The surplus-opportunity detection achieved 91.06% accuracy, and 89.24% of the total LiB charging energy occurred during measured surplus intervals. These results confirm the effectiveness of the weather-forecast-linked energy-management concept for overseas green-base-station deployment.**

***Index Terms*—mobile base station, photovoltaic power, lithium-ion battery, weather forecast, green base station, Philippines**

I. Introduction

The resilience of telecom power systems is particularly important in regions where commercial electricity supply is exposed to reliability constraints. For mobile-network operators, such conditions motivate the development of base-station power systems that can reduce dependence on commercial electricity while maintaining operational continuity.

Solar-powered cellular base stations have been widely discussed as a practical pathway toward greener mobile networks. Chamola and Sikdar reviewed solar-powered cellular base stations and highlighted that renewable-energy deployment must address the mismatch between solar availability, load demand, battery operation, and site reliability requirements [1]. Alsharif *et al.* further summarized green and sustainable cellular base-station architectures, emphasizing renewable energy and storage as key elements for future base-station design [2]. More recent work has also investigated optimal sizing of PV and energy-storage systems for cellular base stations, showing that site-specific PV generation and load profiles strongly affect achievable autonomy and cost performance [3]. These studies establish the importance of PV-battery systems for green telecom infrastructure, but many of them focus on surveys, design, or simulation-based sizing rather than measured field operation of forecast-linked battery scheduling.

A weather-forecast-linked power-control method was previously proposed that adjusts LiB operation in advance according to the next-day weather outlook [4]. When sufficient PV generation is expected, the battery schedule creates SOC headroom before the daytime surplus period. When PV generation is expected to be limited, unnecessary battery discharge is avoided so that available stored energy is retained. This concept is attractive for green base stations because it addresses both renewable-energy utilization and resilience.

The novelty of the present work is the overseas field demonstration and quantitative validation of this forecast-linked control concept in a Philippine PV-assisted mobile-base-station environment. Compared with previous survey, sizing, and simulation studies, this paper evaluates measured PV output, LiB charge/discharge behavior, SOC response, and forecast-based surplus-opportunity accuracy from field logs. The contribution is threefold: 1) to describe the deployed hardware, software, and forecast-linked control flow; 2) to evaluate the PV self-sufficiency improvement and the amount of PV electricity effectively recovered through LiB charging; and 3) to validate whether the forecast-linked surplus prediction identifies the next-day surplus opportunity observed in field measurements, together with the temporal alignment of actual LiB charging with measured surplus periods.

II. Field System and Forecast-Linked Control

A. Hardware Configuration

The field experiment was conducted from 23 April to 18 May 2026 at a site located at $14°28'13''$ N latitude and $121°02'41''$ E longitude. Fig. 1 shows the overall structure of the demonstration system. The field site was equipped with a 7.38 kW PV array, a 6 kW PV converter, a 3840 Ah LiB bank, commercial AC power input, a rectifier with 52.5 V output voltage and 44 A output current, and a 48 V DC distribution path supplying a mobile-base-station load. The reference site load used in the evaluation was approximately 2.31 kW, calculated from the rectifier output voltage and current. The LiB operated bidirectionally, discharging to support the DC

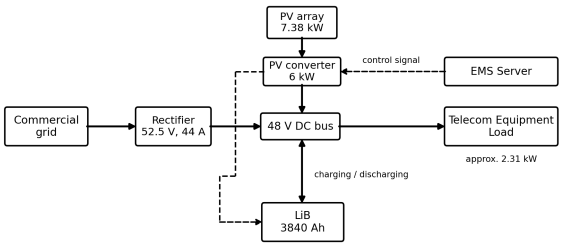

Fig. 1. Overall configuration of the Philippine PV-LiB base-station demonstration system.

TABLE I
MAIN SPECIFICATIONS OF THE DEMONSTRATION SITE

Item	Specification
PV array	7.38 kW
PV converter	6 kW
PV converter voltage	55.5 V
LiB bank	3840 Ah
Rectifier output voltage	52.5 V
Rectifier output current	44 A
Reference telecom load	2.31 kW
Measurement interval	1 min
Evaluation period	26 days

side when scheduled and charging when PV surplus was available.

B. Software Operation

The forecast-linked logic was implemented through an energy-management server. The server collected the weather forecast required for the next operating day at approximately 20:00 Philippine Standard Time (PST). The control code was executed at approximately 20:30 PST and generated the LiB control schedule to be reflected from the following day onward. This separation between forecast acquisition, schedule generation, and next-day control is important because the field response should be interpreted against the scheduled operating day rather than the time at which code execution occurred.

The server also retained operational logs for performance evaluation. The logged variables relevant to this paper include PV output power, LiB charging/discharging power, SOC, and timestamps. Weather forecast data and observed weather data were used as supporting information for control operation and interpretation of PV variability.

C. Forecast-Linked Control Algorithm

The control concept follows the weather-forecast-linked power-control method reported in [4], but was implemented here as an automatic next-day scheduling function for the Philippine field site. Fig. 2 summarizes the control and validation flow. The algorithm is executed once per day after the evening forecast is acquired. It produces a time-sequential control command for the following operating day, rather than making an isolated instantaneous charge/discharge decision.

The first step is forecast acquisition and prediction. The server acquires weather-forecast data for the next operating day. The primary input for PV-surplus prediction is shortwave irradiance, because it is directly related to the expected PV output. Additional forecast variables, including weather type, temperature, relative humidity, cloud cover, wind, rainfall, and precipitation probability, are retained as supporting information for poor-weather and backup-oriented operation. Based on the system specification, the forecast module estimates three quantities at 30-min resolution: PV generation, site load, and expected grid-import energy. The PV-generation forecast is calculated from the irradiance forecast, PV capacity, and a fixed conversion coefficient. The load forecast is obtained from the site-load model and weather-dependent auxiliary demand. The expected grid-import energy is then calculated from the difference between the predicted load and predicted PV generation.

The second step is surplus judgement. For each time interval, the controller compares the forecast-derived PV output with the reference telecom load. In this field evaluation, the reference load was 2.31 kW. A meaningful daytime PV-surplus opportunity is therefore detected when the forecast-derived PV output exceeds this reference load. The forecast-derived surplus energy is calculated as

$$\hat{E}_{\mathrm{surplus}} = \sum_{i} \max(\hat{P}_{\mathrm{PV,i}} - P_{\mathrm{load}}, 0)\Delta t_i \qquad (1)$$

where $\hat{P}_{\mathrm{PV,i}}$ is the forecast-derived PV output in interval i, $P_{\mathrm{load}} = 2.31$ kW, and Δt_i is the interval length. This positive-difference formulation is used to identify whether the next day has enough daytime PV surplus to justify creating LiB charging headroom in advance.

The third step is SOC policy determination. When the forecast indicates sufficient daytime surplus, the controller calculates the amount of LiB headroom required to absorb the expected surplus. The target SOC is set so that the difference between the current SOC and the target SOC corresponds to the required storage headroom, while respecting the lower SOC limit and backup SOC requirement. If the current average SOC is higher than the target SOC, a pre-discharge command is scheduled before the predicted surplus period. If the current average SOC is lower than the target SOC, the system schedules charging to reach the required target SOC. This logic prevents unnecessary deep discharge while still preparing enough headroom for the next-day surplus PV energy.

The fourth step is schedule generation in automatic mode. The generated control command consists of three possible states: standby, discharge, and charge. For a day with predicted surplus, the controller first keeps the LiB in standby or adjusts SOC before the surplus window, then schedules LiB charging during the predicted surplus period. After the predicted surplus window, the controller compares the target SOC with the backup SOC and selects discharge, charge, or standby to maintain the required backup capability. For a day without

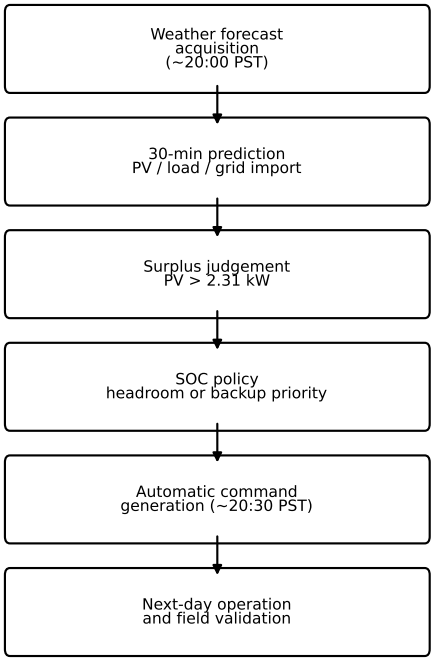

Fig. 2. Forecast-linked control flow based on next-day weather forecasts, 30-min PV/load/grid-import prediction, surplus judgement, SOC policy, automatic control-command generation, and next-day field validation.

predicted surplus, the controller prioritizes backup operation by charging the LiB during the night or early morning and maintaining a higher SOC during the day. The resulting schedule is stored as the automatic control command and is reflected in the following day's operation.

Finally, the field validation compares the forecast-derived surplus opportunity with the measured surplus opportunity and examines whether the actual LiB charging energy was concentrated during measured surplus periods. This validation focuses on the effectiveness of the forecast-linked control basis, not merely on whether the generated command was executed.

D. Acquired Data and Evaluation Method

One-minute field logs from a 26-day demonstration period were used. Let $P_{\mathrm{PV}}(t)$ denote PV output, P_{load} the reference load of 2.31 kW, and $P_{\mathrm{ch}}(t)$ the nonnegative LiB charging power. In a no-LiB counterfactual, the directly usable PV power was limited to $\min(P_{\mathrm{PV}}(t), P_{\mathrm{load}})$. The PV-surplus energy effectively captured by LiB was conservatively estimated as the time integral of the overlap between contemporaneous LiB charging and PV output above the reference load.

The operational PV self-sufficiency index was defined as

$$S_{\mathrm{PV}} = \frac{E_{\mathrm{directPV}} + E_{\mathrm{surplus,LiB}}}{E_{\mathrm{load}}} \tag{2}$$

For the no-LiB counterfactual, $E_{\mathrm{surplus,LiB}} = 0$.

The predictive effect of the forecast-linked control algorithm was evaluated by comparing forecast-derived PV-surplus opportunities with the next-day surplus opportunities realized in field measurements. The forecast-derived PV output used the same control-side conversion concept described in the system design: solar-irradiance forecast values were mapped to PV output using the rated PV capacity and the fixed slope coefficient used by the controller. PV surplus was defined consistently as PV output above the 2.31 kW reference load. Hourly surplus-opportunity detection accuracy was defined as the fraction of hourly intervals for which the predicted surplus state agreed with the measured surplus state. Let $\hat{y}_h$ denote the predicted surplus state in hour h, where $\hat{y}_h = 1$ when the forecast-derived hourly PV output exceeds the 2.31 kW reference load and $\hat{y}_h = 0$ otherwise. Let y_h denote the measured surplus state, where $y_h = 1$ when the hourly mean measured PV output exceeds the 2.31 kW reference load and $y_h = 0$ otherwise. The accuracy was calculated as

$$\mathrm{accuracy} = \frac{TP + TN}{TP + TN + FP + FN} \tag{3}$$

where TP, TN, FP, and FN denote true positive, true negative, false positive, and false negative hourly classifications, respectively. This analysis evaluates whether the forecast-linked control basis anticipates the actual next-day surplus opportunity available for battery charging, rather than whether the generated command schedule is executed as written.

III. Results and Discussion

A. Representative Daily Operation

Fig. 4 presents a representative 24-h trace. PV output increased after sunrise and exceeded the site-load level during the daytime. The LiB power profile shows discharge before the daytime surplus period and charging during the high-PV interval. Positive LiB power denotes charging and negative LiB power denotes discharging. This operating pattern is consistent with the forecast-linked control objective: battery headroom is prepared before surplus PV becomes available and is then used to absorb that surplus energy.

Fig. 5 shows the single-day SOC trajectory for the same date. The shaded interval indicates the PV-surplus period, defined as the interval during which PV output exceeded the 2.31 kW reference load. SOC increased mainly during this interval. Thus, the field data confirm that LiB charging was concentrated in the period when solar power exceeded site demand, rather than being arbitrarily distributed across the day.

B. PV Self-Sufficiency and Recovered Surplus Energy

Table II summarizes the field evaluation. Over the analyzed period, the reference-load energy was 1441.44 kWh. Without LiB storage, the direct PV contribution was 549.32 kWh, corresponding to a PV self-sufficiency index of 38.11%. With LiB-enabled surplus capture, the usable PV-derived energy increased by 332.60 kWh, and the PV self-sufficiency index reached 61.18%. The improvement was therefore 23.07 percentage points.

The 332.60 kWh value can be interpreted as PV electricity that would not have been fully available to the site in the no-LiB counterfactual, because instantaneous PV output exceeded

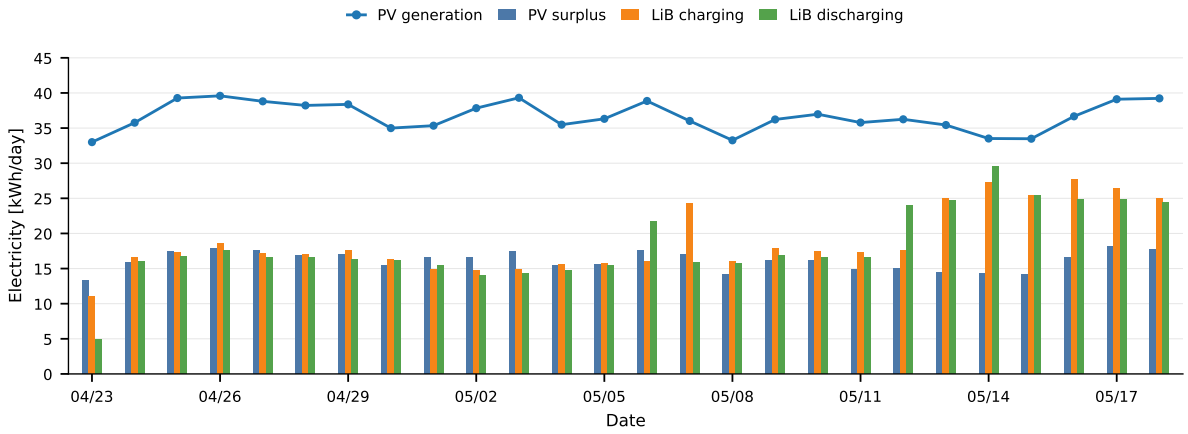

Fig. 3. Daily PV generation, PV surplus, LiB charging energy, and LiB discharging energy over the 26-day demonstration period.

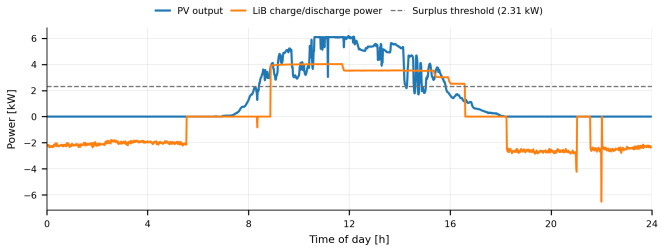

Fig. 4. Representative 24-h profile of PV output and LiB charging/discharging power.

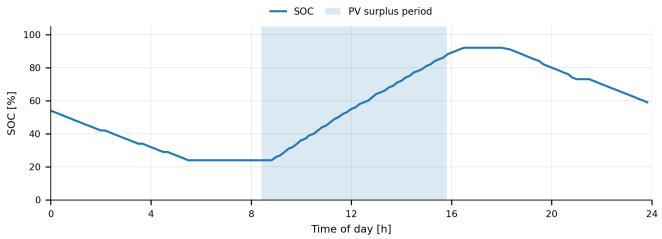

Fig. 5. Single-day SOC trajectory with the PV-surplus period highlighted.

TABLE II
SUMMARY OF FIELD EVALUATION RESULTS

Metric	Result
Reference-load energy	1441.44 kWh
Direct PV contribution without LiB	549.32 kWh
Measured PV surplus above site load	430.51 kWh
PV surplus captured by LiB	332.60 kWh
PV self-sufficiency without LiB	38.11%
PV self-sufficiency with LiB	61.18%
Absolute improvement	23.07 %

the reference load. Compared with prior PV-battery base-station studies that mainly evaluated system feasibility, optimal sizing, or simulated autonomy [1]– [3], the present result provides a measured field estimate of how much surplus PV can be recovered by forecast-linked LiB operation at an operating telecom site. The observed 23.07 percentage-point improvement in PV self-sufficiency is therefore complementary to the design-oriented findings of previous work.

Fig. 3 presents daily PV generation, PV surplus, LiB charging energy, and LiB discharging energy. The recurrent appearance of LiB charging on days with substantial PV generation supports the interpretation that the battery acted as a renewable-energy buffer, rather than only as standby equipment. The simultaneous observation of discharge and recharge across days is also consistent with the intended daily shift of energy availability.

C. Validation of Forecast-Linked Surplus Prediction

The algorithm was designed to estimate the next-day surplus PV opportunity and create battery headroom accordingly. Its predictive validity was therefore assessed against the realized surplus opportunity, rather than against command execution alone. Hourly surplus-opportunity detection accuracy was defined as the fraction of hourly intervals for which the predicted surplus state agreed with the measured surplus state. The forecast-linked surplus-opportunity estimate achieved 91.06% hourly accuracy across 604 paired hourly records, indicating high overall agreement against field measurements.

Field operation further showed that 89.24% of total LiB charging energy occurred during measured surplus intervals. This result confirms that the implemented control converted the predicted surplus opportunity into mostly surplus-aligned charging behavior.

IV. CONCLUSION

A weather-forecast-linked energy-management method was demonstrated at a PV-assisted mobile base station in the Philippines. The system integrated a 7.38 kW PV array, a 3840 Ah LiB bank, and an energy-management server that generated next-day schedules from evening forecast inputs. The reference telecom load was 2.31 kW. Compared with a no-LiB counterfactual, the PV self-sufficiency index increased from 38.11% to 61.18%, while 332.60 kWh of surplus PV was

utilized. Forecast-linked surplus-opportunity detection reached 91.06% hourly accuracy, and 89.24% of total LiB charging energy occurred during measured surplus intervals. These results support the applicability of forecast-linked energy management to green base stations in electricity-reliability-constrained environments.

REFERENCES

[1] V. Chamola and B. Sikdar, "Solar powered cellular base stations: Current scenario, issues and proposed solutions," *IEEE Communications Magazine*, vol. 54, no. 5, pp. 108–114, May 2016.

[2] M. H. Alsharif, J. Kim, and J. H. Kim, "Green and sustainable cellular base stations: An overview and future research directions," *Energies*, vol. 10, no. 5, Art. 587, Apr. 2017.

[3] M. Javidsharifi, S. Spataru, B. Javidsharifi, and D. Sera, "Optimum sizing of photovoltaic and energy storage systems for powering green base stations in cellular networks," *Energies*, vol. 14, no. 7, Art. 1895, Mar. 2021.

[4] M. Nakamura and K. Takeno, "Power control method of mobile base stations using lithium-ion battery and solar power," *IEICE Transactions on Communications*, vol. J100-B, no. 4, pp. 307–314, Apr. 2017.